

Monte Carlo model for the photoluminescence kinetics of a quantum dot embedded in a nanocavity

G. Tarel and **V. Savona**

Institute of Theoretical Physics, Ecole Polytechnique Fédérale de Lausanne EPFL, CH-1015 Lausanne, Switzerland

E-mail: guillaume.tarel@epfl.ch

A. Badolato

Department of Physics and Astronomy, University of Rochester, Rochester, New York 14627, USA

M. Winger, T. Volz, and A. Imamoglu

Institute of Quantum Electronics, ETH Zürich, CH-8093 Zürich, Switzerland

Abstract. We address the problem of the photoluminescence of a quantum (QD) dot in a nanocavity, with focus on the case of nonzero detuning. In this regime, experiments have shown that strong emission from the cavity-like peak is still present for dot-cavity detuning exceeding 10 meV, which seems puzzling. We will discuss the general theory of *cavity feeding*, due to the relaxation and recombination kinetics of a multiply excited QD. We first compute the multi-exciton manifolds using a configuration-interaction scheme, starting from a truncated single-particle basis. We then run Monte-Carlo paths of excitation-emission kinetics on these states. This allows to extract photoluminescence spectra and two-photon correlation curves. The agreement with experimental data [1, 2] is very good. Our result shows unambiguously that the cavity feeding mechanism at large detunings can be attributed to excited-state multiexciton radiative decay (mostly biexcitons), also involving states in the wetting layer continuum.

1. Introduction

Once the strong coupling was achieved for semi-conductor quantum dots (QDs) in micro/nano-cavities [1, 3, 4, 5, 6, 2], an interesting parallel was drawn between cavity quantum electrodynamics (CQED) using atoms or semiconductor QDs. The question however arises, in which terms the solid state system differs from its atomic counterpart. Indeed, as it is now well established, a QD can not be considered as a perfect two level system, due to its efficient coupling to the surrounding semi-conductor (SC) matrix. In particular, this non-ideal behavior leads to an unexpected persistence of a PL peak at the cavity frequency, even for large QD-cavity detuning. Here, we develop a model of excitation-emission kinetics based on multi-exciton manifolds, that we compute from an effective mass model. We show that the emission at the cavity frequency is produced by decays from N- to N-1-exciton manifolds, with the initial state mostly involving continuum states above the QD barrier. The agreement of our results with recent experiments is excellent, especially in predicting two-photon correlations. In this

respect, contrary to many existing models [14, 15, 13], our picture is the only one providing a full quantitative account of spectra and time-correlation functions.

2. Eigenstates of the many-body Hamiltonian

We compute the single particle states in the QD by using an effective mass description, restricting to one electron and one heavy hole band. To account for the finite height of the QD barriers – giving rise to the 2D extended states of the wetting layer – we use a truncated parabolic potential, with frozen z-motion. Features such as the precise QD shape, strain, etc., are purposely not accounted for, as they would only produce a quantitative effect on the principal mechanism that we are describing. Single-particle states are sketched in Fig. 1. The sets of single-particle states are truncated, including 18 electron, 32 holes states, and their spin degrees of freedom. Most of these single-particle states are extended states in the wetting layer. Accounting for these states is essential, as they will result in a quasi-continuum of excited multi-exciton states, allowing to match the transition frequency corresponding to the cavity mode. This feature has no counterpart in CQED of atoms, and rules out simple two-level models often adopted for modeling QD spectra.

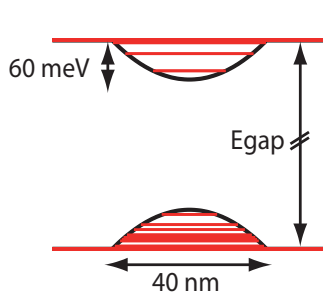


Figure 1. Single electron/holes states, calculated in a truncated parabolic potential.

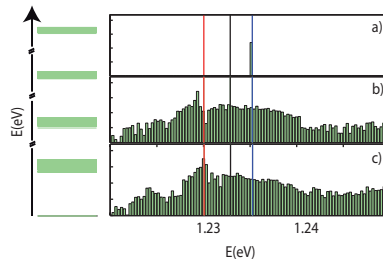


Figure 2. Left: Multiexcitonic states – Right: joint density of states for a) 1X manifold to ground state b) 2X manifold to 1X manifold c) 3X to 2X

We now compute eigenstates of the Coulomb hamiltonian including extended multiexcitonic states. For this, we start from the Hartree-Fock configurations of n electron-hole pairs, thus neglecting charged states. We will use these configurations as a basis for the configuration interaction calculation of the Coulomb correlated eigenstates [9, 10, 16]. The Coulomb Hamiltonian is

$$H = \sum_i \epsilon_i \hat{c}_i^\dagger \hat{c}_i + \sum_j \epsilon_j \hat{d}_j^\dagger \hat{d}_j + \frac{1}{2} \sum_{i_1, i_2, i_3, i_4} V_{i_1, i_2, i_3, i_4} \hat{c}_{i_1}^\dagger \hat{c}_{i_2}^\dagger \hat{c}_{i_3} \hat{c}_{i_4} + \frac{1}{2} \sum_{j_1, j_2, j_3, j_4} V_{j_1, j_2, j_3, j_4} \hat{d}_{j_1}^\dagger \hat{d}_{j_2}^\dagger \hat{d}_{j_3} \hat{d}_{j_4} - \sum_{i_1, i_2, j_1, j_2} V_{i_1, j_1, i_2, j_2} \hat{c}_{i_1}^\dagger \hat{d}_{j_1}^\dagger \hat{d}_{j_2} \hat{c}_{i_2}. \quad (1)$$

We compute more than 2000 multiexcitonic states, including spin, up to the four-exciton multiplet (see Fig. 2, left part). In the right panel of this figure is the computed joint density of states for the QD. While for the one electron-hole pair multiplet (excitonic multiplet), the only accessible transition is the X0, there is a large DOS for transitions from multiexcitonic manifolds (at least 2nd multiplet) to the next downwards. For a QD in a uniform medium, these transitions will only provide a broad background to the PL spectrum: a PL measurement would show an ensemble of distinct peaks originating from X0, XX0 etc., superposed to a broad background. In presence of a resonant cavity, the transitions resonant with the cavity mode will be enhanced by Purcell effect, thus feeding the emission at the cavity frequency.

3. Monte-Carlo simulation

To prove that the emission background is actually able to feed the cavity efficiently, we use a Monte-Carlo method to simulate the continuous-wave PL under non-resonant excitation. We compute the rates of all processes starting from any level and ending in any other level. The first process we account for, is the capture process from a multiexciton manifold $N-X$ to the next manifold $(N+1)-X$, by absorption of an additional electron hole pair. This process models the capture, in the multi-exciton states under study, of an electron-hole pair produced by the excitation laser in higher-lying states of the semiconductor. The second process is the radiative decay, that we model including the Purcell factor implied by the cavity resonance. Finally, inside each multiplet, relaxation mechanism through optical phonon are modeled as in Ref. [8]. In addition, we have to account for a spin-flip process, which we treat as a quasi resonant process with a lifetime of $\approx 100ps$. For all these process we compute the transition rates, starting from appropriate Hamiltonians in the electron-hole basis.

4. Results

The Monte-Carlo simulation gives access to both PL spectra and two-time correlation functions, as measured in a Hanbury-Brown and Twiss experiment. The simulated PL spectrum is shown in Fig. 3. For this 5nm red detuned device, a cavity peak (C) is always visible together with the usuals X0 and XX0 peaks (blue and black arrow). This is a first evidence that our model can explain the cavity feeding mechanism. In addition, we can simulate two time correlations ($g^2(\tau)$) curves. Fig. 4 shows the simulated curves for the exciton-exciton, cavity-cavity, and exciton-biexciton correlations, and the corresponding measured ones. For the cavity-cavity correlation, we observe that the measured $g^2(0)$ is significantly lower than in the calculations. We attribute this difference to the absence of charged excitons in our model. In any case, our explanation in terms of multiexcitons is perfectly compatible with the sub-poissonian nature of this curve, due to the possibility of cavity photon cascades. Further validation of the cavity feeding mechanism

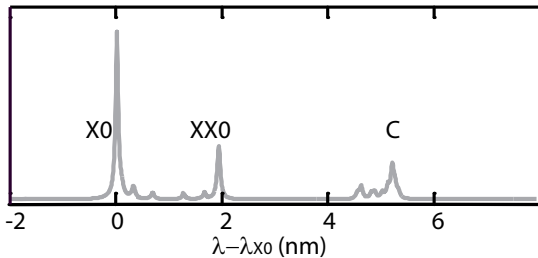


Figure 3. Computed PL spectrum for a red detuned device. For this detuning of 5nm, a peak at the cavity frequency (C) is visible.

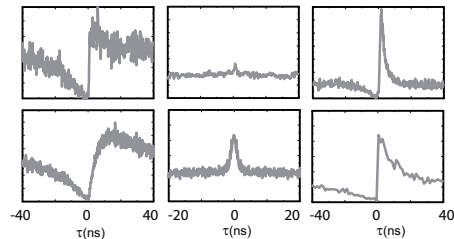


Figure 4. Measured (top) and calculated (bottom) $g^2(\tau)$ time correlations. From left to right: cavity-exciton, cavity-cavity, and exciton-biexciton correlations.

comes from the analysis of the power dependence of the spectrum (see Fig. 5). While the X0 and XX0 peaks saturate at high excitation power, as expected, the cavity peak does not saturate within the considered power range. This feature is explained as the cavity feeding involves transitions from high multi-exciton manifolds, that are expected to saturate at higher power. In addition, for low pump power the cavity peak shows a superlinear power dependence, again due to the multi-excitonic origin of the cavity feeding. Both the power dependence of the cavity PL and the two-photon correlations have been demonstrated in experiments. They are a natural consequence of the assumptions of our model. On the contrary, they cannot be explained by any model that assumes PL originating from a single exciton level [13, 14, 15] – no matter how

spectrally shaped – that would imply linear power dependence, saturation similar to the exciton line, and antibunched emission at the cavity frequency whatever the excitation power.

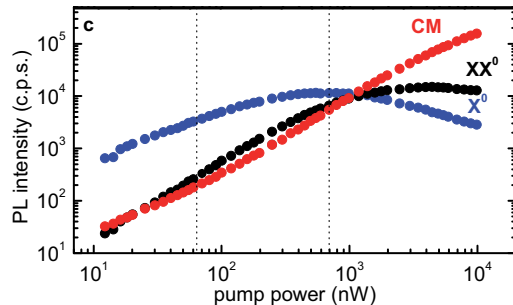


Figure 5. Measured PL intensity as a function of the pump power X_0 , XX_0 and cavity peak.

5. Conclusion

Our simulations clearly show that multiexcitonic manifolds are an unavoidable ingredient for the explanation of the cavity feeding mechanism at large detuning. In a typical experiment, given the small QD size and the minimum power required to detect any PL signal, the QD is always in a highly excited state, where multiexcitons are excited during a considerable fraction of time. In computing multiexcitonic states and including them in our dynamic model, we are able to explain all the observations related to the cavity feeding mechanism: the surviving cavity PL at large detuning, the second order time correlation curves and the power dependence.

Acknowledgments

We thank K. Hennessy and E. Hu for their contribution in the samples processing, J. Finley and A. Beveratos for their contribution to the elaboration of the model and S. Portolan for support regarding the Monte-Carlo simulations. We would also like to thank Wolfgang Langbein for enlightening discussions. This work is supported by NCCR Quantum Photonics (NCCR QP), research instrument of the Swiss National Science Foundation (SNSF).

References

- [1] K. Hennessy et al., *Nature*, vol. 445, p.896-899 (2007).
- [2] M. Kaniber et al., *Phys. Rev. B.*, vol. 77, p.161303-+ (2008).
- [3] T. Yoshie et al., *Nature*, vol. 432, p.200-203 (2004).
- [4] E. Peter et al., *Phys. Rev. Lett.*, vol. 95, 067401 (2005).
- [5] J.P. Reithmaier et al., *Nature*, vol. 432, p.197-200 (2004).
- [6] K. Srinivasan and O. Painter, *Nature*, vol.450, p.862-866 (2007).
- [7] S. Strauf et al., *Phys. Rev. Lett.*, vol. 96, 127404 (2006).
- [8] T. Grange et al., *Phys. Rev. B*, vol. 96, 241304(R) (2007).
- [9] E. Biolatti et al., *Phys. Rev. B.*, vol. 65, 075306 (2002).
- [10] A. Barenco et M. A. Dupertuis, *Phys. Rev. B*, vol. 52, 2766 (1995).
- [11] C. Jacoboni and L. Reggiani, *Rev. Mod. Phys.*, vol. 55, 645 (2003).
- [12] M. Grundmann and D. Bimberg, *Phys. Rev. B*, vol. 55, 9740 (1997).
- [13] A. Naesby et al., *Phys. Rev. A*, vol. 78, 045802 (2008).
- [14] A. Auffèves et al., *Phys. Rev. A*, vol. 79, 053838 (2009).
- [15] J. Suffczynski et al., *Arxiv*, arXiv: 0904.0271 (2009).
- [16] W. Sheng and P. Hawrylak, *Phys. Rev. B.*, vol. 72, 035326 (2005).